



Fermi National Accelerator Laboratory

FERMILAB-Conf-88/184-T

November, 1988

Heavy Quark Production at Collider Energies¹

R. K. Ellis

Fermi National Accelerator Laboratory

P.O. Box 500, Batavia, Illinois 60510, USA

Abstract

I review the theory of heavy quark production in QCD at collider energies. The most important features of the recently published results on higher order corrections to the heavy quark production cross-section are described. The phenomenological consequences of these formulae for bottom and top quark production at $S\bar{p}\bar{p}S$ and Tevatron energies are presented.

¹Invited talk presented at the 7th Topical Workshop on Proton-Antiproton Collider Physics, Fermilab, 20-24 June 1988.



1. Introduction

In this paper I review the status of the theory of heavy quark production. The production of heavy quarks in hadron-hadron collisions continues to be a topic of great theoretical interest. The reasons for this enthusiasm are the existence of much experimental data on charm production and the recent publication of data on bottom quark production in hadronic reactions. For a review of the data on the hadroproduction of heavy quarks at fixed target energies I refer the reader to ref. [1]. An additional motivation is provided by the need to relate the results of the search for the top quark[2] to a value of the heavy quark mass.

In the hadroproduction of heavy quarks there are two incoming strongly interacting particles. The produced quarks are coloured objects which subsequently fragment into the heavy mesons and baryons observed in the laboratory. Therefore heavy quark production is an important check of the QCD improved parton model in a complex hadronic environment. Because of their semi-leptonic decays, heavy quarks give rise to electrons, muons and neutrinos. Prompt leptons and missing energy are often used as signals for new phenomena. An accurate understanding of heavy quark production cross-sections is necessary to calculate background rates in the search for new physics.

The standard perturbative QCD formula for the inclusive hadroproduction of a heavy quark Q of momentum p and energy E ,

$$H_A(P_1) + H_B(P_2) \rightarrow Q(p) + X \quad (1.1)$$

determines the invariant cross-section as follows,

$$\frac{E d^3\sigma}{d^3p} = \sum_{i,j} \int dx_1 dx_2 \left[\frac{E d^3\hat{\sigma}_{ij}(x_1 P_1, x_2 P_2, p, m, \mu)}{d^3p} \right] F_i^A(x_1, \mu) F_j^B(x_2, \mu). \quad (1.2)$$

The functions F_i are the number densities of light partons (gluons, light quarks and antiquarks) evaluated at a scale μ . The symbol $\hat{\sigma}$ denotes the short distance cross-section from which the mass singularities have been factored. Since the sensitivity to momentum scales below the heavy quark mass has been removed, $\hat{\sigma}$ is calculable as a perturbation series in $\alpha_S(\mu^2)$. The scale μ is *a priori* only determined to be of the order of the mass m of the produced heavy quark. Variations in the scale μ lead to a considerable uncertainty in the predicted value of the cross-section. This uncertainty is diminished when higher order corrections are included.

The theoretical justification for the use of Eq. (1.2) in heavy quark production has been discussed in refs. [3, 4]. Although there is no proof of factorisation in heavy quark production, arguments based on the examination of low order graphs suggest that factorisation will hold. No flavour excitation contributions are included in Eq. (1.2), since the sum over partons runs only over light partons. Graphs having the same structure as flavour excitation are included as higher order corrections. Interactions with spectator partons give rise to terms not shown in Eq. (1.2) which are suppressed by powers of the heavy quark mass. These power corrections should be suppressed relative to the leading order by $(\Lambda/m)^2$. Note however that in ref. [5] a non-relativistic calculation has been performed which finds terms which are only suppressed by (Λ/m) . It would be useful (particularly in the interpretation of charm data) to establish that the power corrections in the full relativistic theory are in fact $(\Lambda/m)^2$.

The lowest order parton processes leading to the hadroproduction of a heavy quark Q are shown in Fig. 1,

$$\begin{aligned} (a) \quad q(p_1) + \bar{q}(p_2) &\rightarrow Q(p_3) + \bar{Q}(p_4) \\ (b) \quad g(p_1) + g(p_2) &\rightarrow Q(p_3) + \bar{Q}(p_4). \end{aligned} \quad (1.3)$$

The four momenta of the partons are given in brackets. The invariant matrix elements squared for processes (a) and (b) have been available in the literature for some time[6, 7, 8] and are given by,

$$\overline{\sum} |M^{(a)}|^2 = \frac{g^4 V}{2N^2} \left(\tau_1^2 + \tau_2^2 + \frac{\rho}{2} \right) \quad (1.4)$$

$$\overline{\sum} |M^{(b)}|^2 = \frac{g^4}{2VN} \left(\frac{V}{\tau_1 \tau_2} - 2N^2 \right) \left(\tau_1^2 + \tau_2^2 + \rho - \frac{\rho^2}{4\tau_1 \tau_2} \right) \quad (1.5)$$

where the dependence on the $SU(N)$ colour group is shown explicitly, ($V = N^2 - 1$, $N = 3$) and m is the mass of the produced heavy quark Q . The matrix elements squared in Eqs. (1.4) and (1.5) have been summed and averaged over initial and final colours and spins. For brevity we have introduced the following notation,

$$\tau_1 = \frac{p_1 \cdot p_3}{p_1 \cdot p_2}, \quad \tau_2 = \frac{p_2 \cdot p_3}{p_1 \cdot p_2}, \quad \rho = \frac{2m^2}{p_1 \cdot p_2}. \quad (1.6)$$

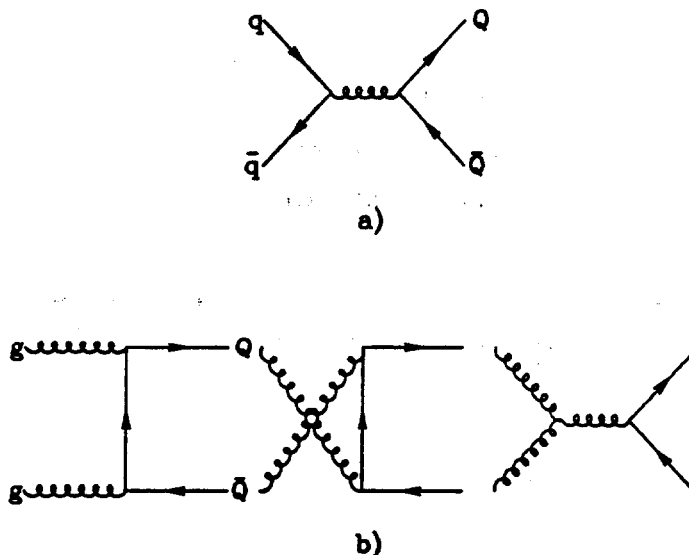


Figure 1: Lowest order processes for heavy quark production.

In terms of these lowest order matrix elements the invariant cross-section at the parton level can be written as,

$$\frac{E_3 d^3\hat{\sigma}}{d^3p_3} = \frac{1}{16\pi^2 s^2} \sum |M|^2 \quad (1.7)$$

where s is the square of the total parton centre of mass energy.

The phenomenological consequences of the lowest order formulae can be summarised as follows. The average transverse momentum of the heavy quark or antiquark is of the order of its mass and the p_T distribution falls rapidly to zero as p_T becomes larger than the heavy quark mass. The rapidity difference between the produced quark and antiquark is predicted to be of order one. The theoretical arguments summarised above do not address the issue of whether the charmed quark is sufficiently heavy that the hadroproduction of charmed hadrons in all regions of phase space is described by the QCD parton model, neglecting terms suppressed by powers of the charmed quark mass. For the application of these formulae to heavy quark production at fixed target energy see ref. [9] and references therein.

There are arguments[10] which suggest that higher order corrections to heavy quark production could be large. These are mostly due to the observation that the

fragmentation process,

$$g + g \rightarrow g + g \quad (1.8)$$

$$\quad \quad \quad \downarrow$$

$$\quad \quad \quad Q + \bar{Q}$$

although formally of order α_S^3 , can be numerically as important as the lowest order $O(\alpha_S^2)$ cross section. This happens because the lowest order cross section for the process $gg \rightarrow q\bar{q}$ is about a hundred times smaller than the cross section for $gg \rightarrow gg$. A gluon jet will fragment into a pair of heavy quarks only a fraction $\alpha_S(m^2)/2\pi$ of the time. Because of the large cross-section for the production of gluons, the gluon fragmentation production process is still competitive with the production mechanisms of Eq. (1.3). The description of heavy quark production by the gluon fragmentation mechanism alone is appropriate only when the produced heavy quark is embedded in a high energy jet[11].

The matrix elements squared for the hadroproduction of a heavy quark pair plus a light parton have all been calculated[10, 8, 12, 13]. By themselves, they have physical significance only when the jet associated with the light parton has a large transverse momentum. When the produced light parton has small transverse momentum the matrix elements contain collinear and soft divergences, which cancel only when the virtual corrections are included, and the factorisation procedure is carried out. Corresponding results for the photoproduction of heavy quarks are given in ref. [14].

A partial $O(\alpha_S^3)$ calculation involving the quark gluon fusion process which is free from soft gluon singularities, but contains collinear singularities has been presented in ref. [8]. This calculation provides a concrete example of the factorisation scheme. However this calculation is valid when the quark gluon process dominates over the competing processes. In other regions one cannot use any partial calculation of higher order effects; both real and virtual diagrams contribute. They separately contain divergences which cancel in a complete calculation.

A full calculation of the inclusive cross section for heavy quark production to order α_S^3 is described in ref. [15]. Some aspects of this calculation are discussed in section 2. A partial check of the results of ref. [15] for the gluon-gluon subprocess has been obtained in ref. [16]. Corresponding results for photoproduction to order $\alpha_S^2\alpha_{em}$ are given in ref [17].

2. Theoretical results

The basic quantities calculated in ref. [15] are the short distance cross sections $\hat{\sigma}$ for the inclusive production of a heavy quark of transverse momentum p_T and rapidity y . This requires the calculation of the cross-sections for the following parton inclusive processes,

$$\begin{aligned} g + g &\rightarrow Q + X, & q + \bar{q} &\rightarrow Q + X, & g + q &\rightarrow Q + X, & g + \bar{q} &\rightarrow Q + X \\ g + g &\rightarrow \bar{Q} + X, & q + \bar{q} &\rightarrow \bar{Q} + X, & g + \bar{q} &\rightarrow \bar{Q} + X, & g + q &\rightarrow \bar{Q} + X. \end{aligned} \quad (2.1)$$

The inclusive cross-sections for the production of an anti-quark \bar{Q} differ from those for the production of a quark Q at a given y and p_T . This interference effect, which first arises in $O(\alpha_S^3)$, is small in most kinematic regions. From these results and Eq. (1.2) we can calculate the distributions in rapidity and transverse momentum of produced heavy quarks correct through $O(\alpha_S^3)$. At this point we list the parton sub-processes which contribute to the inclusive cross-sections.

$$\begin{aligned} q + \bar{q} &\rightarrow Q + \bar{Q}, & \alpha_S^2, \alpha_S^3 \\ g + g &\rightarrow Q + \bar{Q}, & \alpha_S^2, \alpha_S^3 \\ q + \bar{q} &\rightarrow Q + \bar{Q} + g, & \alpha_S^3 \\ g + g &\rightarrow Q + \bar{Q} + g, & \alpha_S^3 \\ g + q &\rightarrow Q + \bar{Q} + q, & \alpha_S^3 \\ g + \bar{q} &\rightarrow Q + \bar{Q} + \bar{q}, & \alpha_S^3. \end{aligned} \quad (2.2)$$

Note the necessity of including both real and virtual gluon emission diagrams in order to calculate the full $O(\alpha_S^3)$ cross-section.

In order to describe the results in a relatively concise way, I concentrate on the calculation of the total cross section for the inclusive production of a heavy quark pair. Integrating Eq. (1.2) over the momentum p we obtain the total cross section for the production of a heavy quark pair,

$$\sigma(S) = \sum_{i,j} \int dx_1 dx_2 \hat{\sigma}_{ij}(x_1 x_2 S, m^2, \mu^2) F_i^A(x_1, \mu) F_j^B(x_2, \mu) \quad (2.3)$$

where S is the square of the centre of mass energy of the colliding hadrons A and B . The total short distance cross section $\hat{\sigma}$ for the inclusive production of a heavy quark from partons i, j can be written as,

$$\hat{\sigma}_{ij}(s, m^2, \mu^2) = \frac{\alpha_S^2(\mu^2)}{m^2} f_{ij}\left(\rho, \frac{\mu^2}{m^2}\right) \quad (2.4)$$

with $\rho = 4m^2/s$, and s the square of the partonic centre of mass energy. μ is the renormalisation and factorisation scale. In ref. [15] a complete description of the functions f_{ij} including the first non-leading correction was presented. These may be used to calculate heavy quark production at any energy and heavy quark mass.

Eq. (2.4) completely describes the short distance cross-section for the production of a heavy quark of mass m in terms of the functions f_{ij} , where the indices i and j specify the types of the annihilating partons. The dimensionless functions f_{ij} have the following perturbative expansion,

$$f_{ij}\left(\rho, \frac{\mu^2}{m^2}\right) = f_{ij}^{(0)}(\rho) + 4\pi\alpha_S(\mu^2) \left[f_{ij}^{(1)}(\rho) + \bar{f}_{ij}^{(1)}(\rho) \ln\left(\frac{\mu^2}{m^2}\right) \right] + O(\alpha_S^2). \quad (2.5)$$

In order to calculate the f_{ij} in perturbation theory we must perform both renormalisation and factorisation of mass singularities. The subtractions required for renormalisation and factorisation are done at mass scale μ . The dependence on μ is shown explicitly in Eq. (2.5). The energy dependence of the cross-section is given in terms of the ratio ρ ,

$$\rho = \frac{4m^2}{s}, \quad \beta = \sqrt{1 - \rho}. \quad (2.6)$$

The running of the coupling constant α_S is determined by the renormalisation group,

$$\frac{d\alpha_S(\mu^2)}{d \ln \mu^2} = -b_0\alpha_S^2 - b_1\alpha_S^3 + O(\alpha_S^4), \quad \alpha_S = \frac{g^2}{4\pi}, \quad b_0 = \frac{(33 - 2n_f)}{12\pi}, \quad b_1 = \frac{(153 - 19n_f)}{24\pi^2} \quad (2.7)$$

where n_f is the number of light flavours.

The quantities $f^{(1)}$ depend on the scheme used for renormalisation and factorisation. Our results are obtained in an extension of the \overline{MS} renormalisation and factorisation scheme. Full details are given in ref. [15]. In this scheme heavy quarks are decoupled at low energy. The light partons continue to obey the same renormalisation group equation as they would have done in the absence of the heavy quarks. Thus our results should be used in conjunction with the running coupling as defined

in Eq.(2.7) and together with light parton densities evolved using the two loop \overline{MS} evolution equations.

The functions $f_{ij}^{(0)}$ defined in Eqs. (2.4,2.5) are;

$$\begin{aligned} f_{q\bar{q}}^{(0)}(\rho) &= \frac{\pi\beta\rho}{27} \left[2 + \rho \right] \\ f_{gg}^{(0)}(\rho) &= \frac{\pi\beta\rho}{192} \left[\frac{1}{\beta}(\rho^2 + 16\rho + 16) \ln \left(\frac{1+\beta}{1-\beta} \right) - 28 - 31\rho \right] \\ f_{gq}^{(0)}(\rho) &= f_{qg}^{(0)}(\rho) = 0. \end{aligned} \quad (2.8)$$

We now turn to the higher order corrections in Eq.(2.5) which are separated into two terms. The $\bar{f}^{(1)}(\rho)$ terms are the coefficients of $\ln(\mu^2/m^2)$ and are determined by renormalisation group arguments from the lowest order cross-sections,

$$\bar{f}_{ij}^{(1)}(\rho) = \frac{1}{8\pi^2} \left[4\pi b_0 f_{ij}^{(0)}(\rho) - \int_{\rho}^1 dz_1 f_{kj}^{(0)}\left(\frac{\rho}{z_1}\right) P_{ki}(z_1) - \int_{\rho}^1 dz_2 f_{ik}^{(0)}\left(\frac{\rho}{z_2}\right) P_{kj}(z_2) \right]. \quad (2.9)$$

P_{ij} are the lowest order Altarelli-Parisi kernels. The quantities $f^{(1)}$ in Eq.(2.5) can only be obtained by performing a complete $O(\alpha_s^3)$ calculation. We do not have exact analytical results for the quantities $f^{(1)}$. In ref. [15] a physically motivated fit to the numerically integrated result is given. The fit agrees with the numerically integrated result to better than 1%. The functions $f^{(0)}$, $f^{(1)}$ and $\bar{f}^{(1)}$ are shown plotted in Figs. 2, 3 and 4 for the cases of quark-antiquark, gluon-gluon and gluon-quark fusion respectively. Notice the strikingly different behaviour of the gluon-gluon and gluon-quark higher order terms in the high energy limit, $\rho \rightarrow 0$. These latter processes allow the exchange of a spin one gluon in the t -channel and are therefore dominant in the high energy limit. These cross sections tend to a constant at high energy. The lowest order terms involve fermion t -channel exchange and therefore fall off at large s as can be seen from Figs. 2 and 3. At high energy I find that[18],

$$\begin{aligned} f_{gg}^{(1)} &\rightarrow 2Nk_{gg} + O(\rho \ln^2 \rho), & \bar{f}_{gg}^{(1)} &\rightarrow 2N\bar{k}_{gg} + O(\rho \ln^2 \rho) \\ f_{gq}^{(1)} &\rightarrow \frac{V}{2N}k_{gq} + O(\rho \ln^2 \rho), & \bar{f}_{gq}^{(1)} &\rightarrow \frac{V}{2N}\bar{k}_{gq} + O(\rho \ln^2 \rho) \end{aligned} \quad (2.10)$$

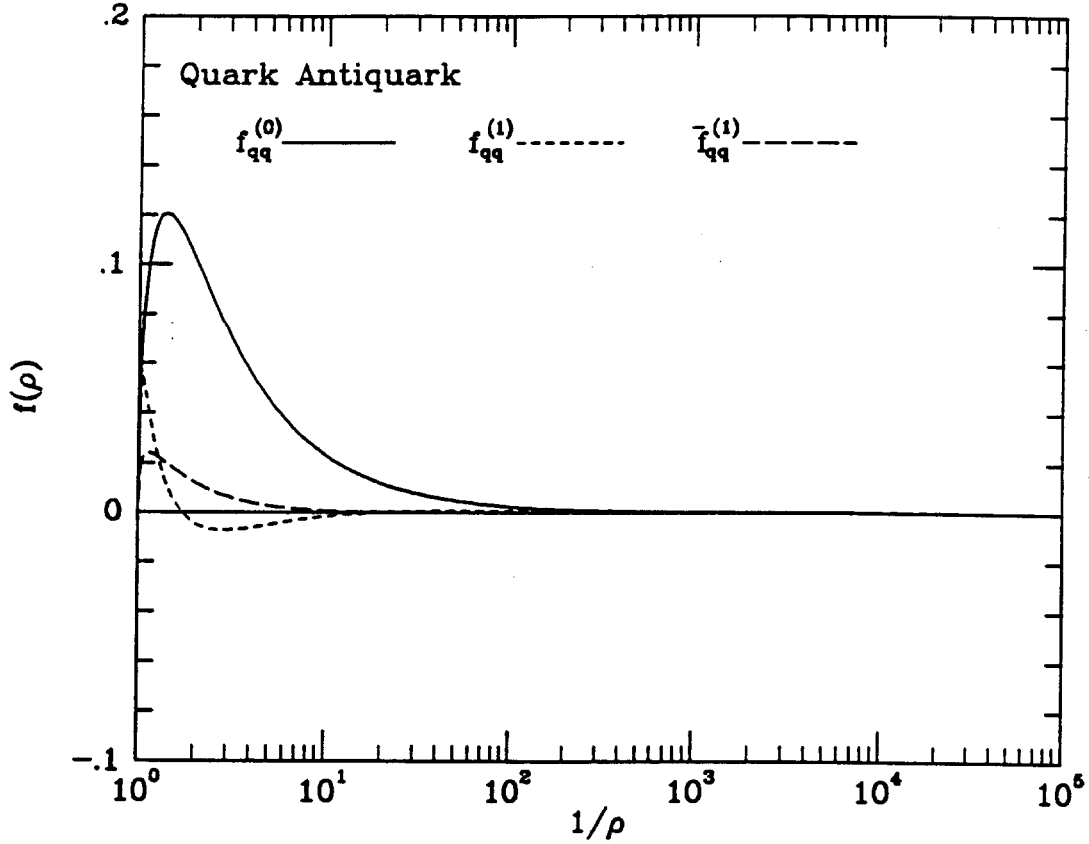


Figure 2: The quark-antiquark contributions to the parton cross section.

where the constants k_{gg} and \bar{k}_{gg} are,

$$\begin{aligned}
 k_{gg} &= \frac{1}{\pi V} \left(\frac{V}{2N} \frac{41}{108} - N \frac{793}{43200} \right) \approx 0.018 \\
 \bar{k}_{gg} &= -\frac{1}{\pi V} \left(\frac{V}{2N} \frac{7}{36} - N \frac{11}{360} \right) \approx -0.0067
 \end{aligned} \tag{2.11}$$

The colour factors V and N are defined after Eq. 1.5. The dominant diagrams are shown in Fig. 5. The asymptotic values of $f_{gg}^{(1)}$ and $f_{gq}^{(1)}$ are proportional to the colour charge of the line which provides the exchanged gluon, since in this limit the upper blob in Fig. 5 is the same for both diagrams and the lower vertex can be approximated by the eikonal form. In the gluon-gluon sub-process the exchanged spin one gluon can come from either incoming gluon, whereas in the gluon quark subprocess it can

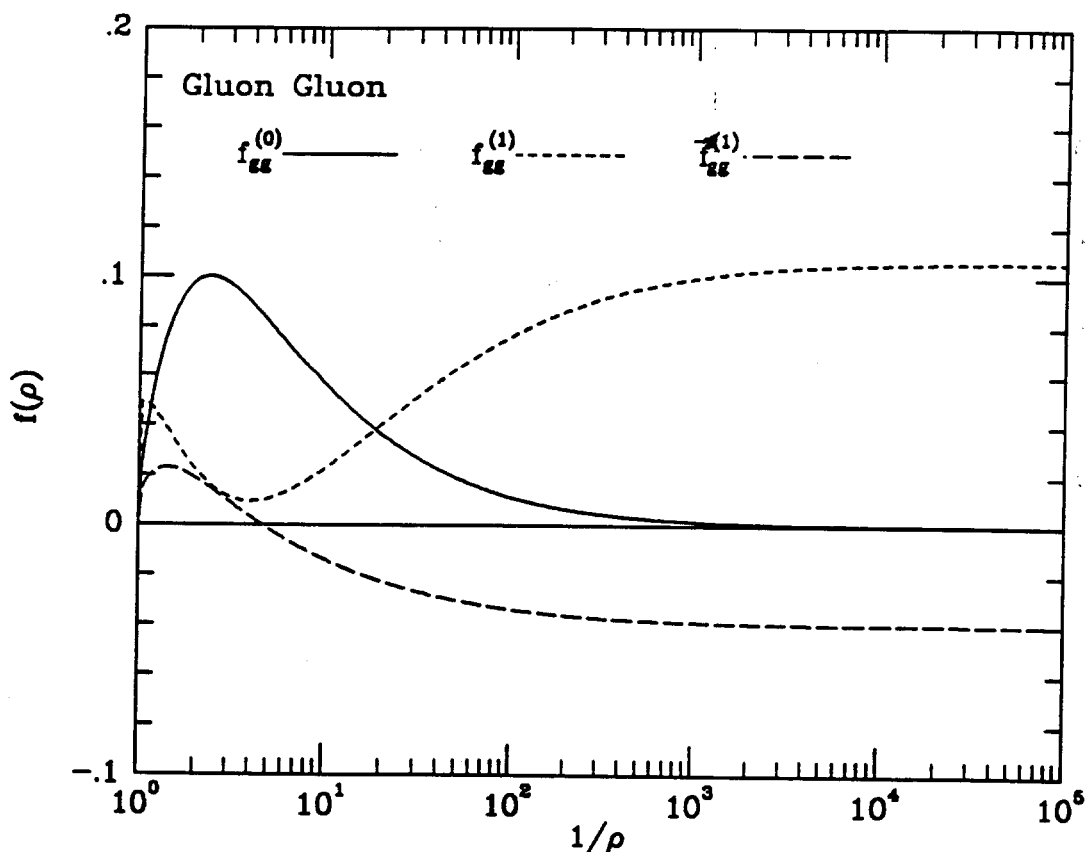


Figure 3: The gluon-gluon contributions to the parton cross section.

only come from the incoming quark line. This, together with the ratio of the gluon and quark charges, explains the relative factor of $9/2$, shown in Eq.(2.10) and evident in Figs. 3 and 4.

A preliminary idea of the size of the corrections can be obtained from Figs. 2, 3 and 4 even before folding with the parton distribution functions. Taking a typical value for $\alpha_s \approx 0.15$, we see that the radiative corrections are large, particularly in the vicinity of the threshold. The significance of the constant cross-section region (gg, gq) at high energy will depend on the rate of fall-off of the structure functions with which the partonic cross-section must be convoluted.

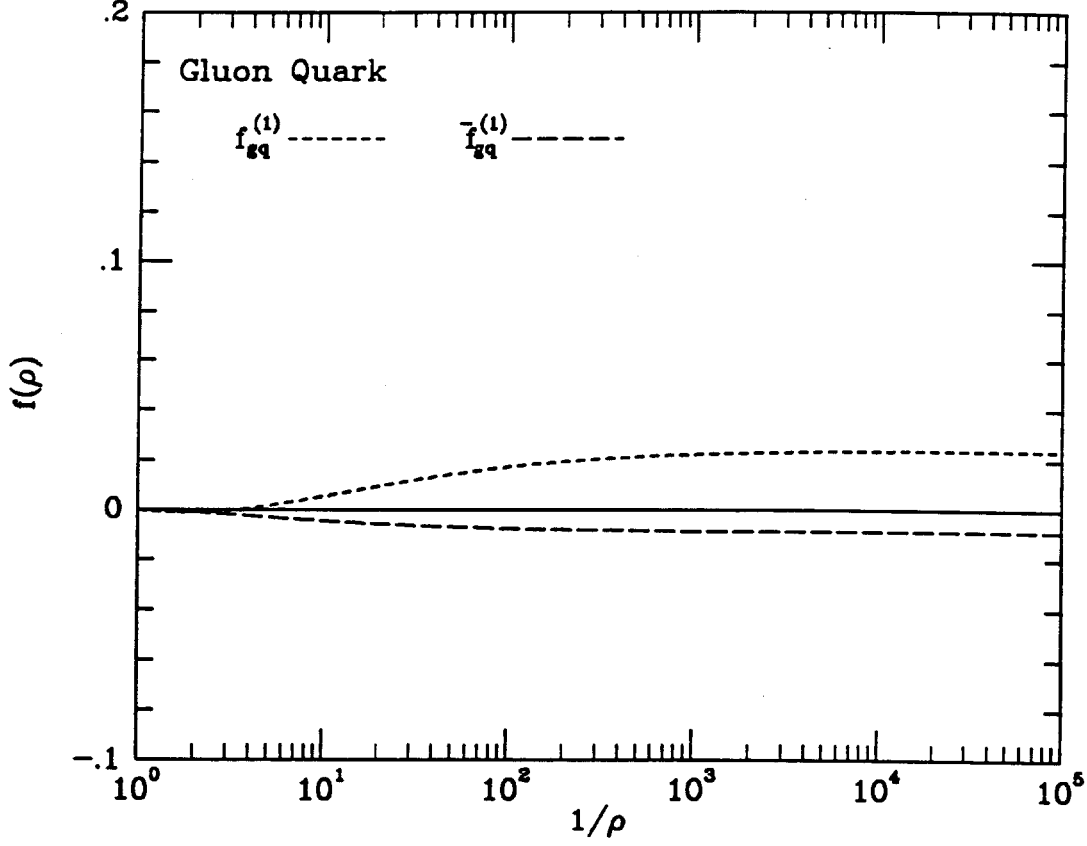


Figure 4: The gluon-quark contributions to the parton cross section.

Near threshold, ($\beta \rightarrow 0$), we have,

$$\begin{aligned}
 f_{q\bar{q}}^{(1)} &\rightarrow \mathcal{N}_{q\bar{q}} \left[-\frac{\pi^2}{6} + \beta \left(\frac{16}{3} \ln^2(8\beta^2) - \frac{82}{3} \ln(8\beta^2) \right) + O(\beta) \right] \\
 f_{gg}^{(1)} &\rightarrow \mathcal{N}_{gg} \left[\frac{11\pi^2}{42} + \beta \left(12 \ln^2(8\beta^2) - \frac{366}{7} \ln(8\beta^2) \right) + O(\beta) \right] \\
 f_{gq}^{(1)} &\rightarrow O(\beta).
 \end{aligned} \tag{2.12}$$

The normalisation, \mathcal{N}_{ij} of the expressions in Eq.(2.12) is determined as follows,

$$\mathcal{N}_{ij} = \frac{1}{8\pi^2} \frac{f_{ij}^{(0)}(\rho)}{\beta} \Big|_{\beta=0}, \quad \mathcal{N}_{q\bar{q}} = \frac{1}{72\pi}, \quad \mathcal{N}_{gg} = \frac{7}{1536\pi}. \tag{2.13}$$

Notice that in this order in perturbation theory the cross-section is finite at threshold.

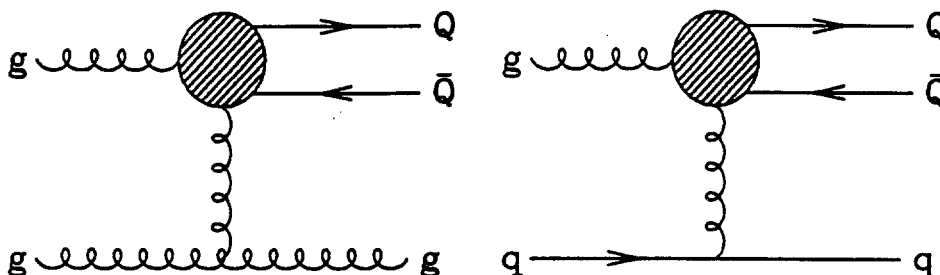


Figure 5: The classes of diagrams responsible for the constant behaviour of the parton cross-section.

This is due to the $1/\beta$ singularity which is responsible for the binding in a coulomb system. The coulomb attraction tends to increase the cross-section when the incoming partons are in a singlet state (gg), and decrease the cross-section when the incoming partons are in an octet state ($gg, q\bar{q}$). This results in a net positive term for the gg case. Note that the numerical importance of the term due to the coulomb singularity is quite small.

We now examine the region near threshold in more detail. The terms in Eq.(2.12) which are finite at threshold have already been explained. The $\ln^2(\beta^2)$ terms in Eq. (2.12) have a general origin. They are due to terms of the form

$$f^{(1)}(\rho) \sim \frac{1}{8\pi^2} \int_{\rho}^1 dz \left[\frac{\ln(1-z)}{1-z} \right]_+ f^{(0)}(\rho/z) \quad (2.14)$$

For attempts to resum these terms of this form in Drell-Yan processes we refer the reader to ref. [19].

3. The total cross-section

In this section I present the results on the total cross-section including the $O(\alpha_s^3)$ results of ref. [15]. Before making phenomenological predictions I shall make an assessment of the theoretical error induced by the uncertainties in the input parameters. The most important uncertainties are the dependence on the choice of scale μ , the uncertainty due to variations of the strong coupling constant and the coupled uncertainty in the parton distribution functions, especially the gluon distribution function.

The gluon distribution function, which is normally extracted from an analysis of scaling violation in Deep Inelastic scattering, introduces a large error. There is a correlation between the form of the gluon distribution function and the value of the running coupling α_s or equivalently the QCD parameter Λ . I shall use a range for the parameter Λ and the associated gluon distributions as given in ref. [20].

The running coupling constant is specified in terms of the Λ parameter by the following formula,

$$\alpha_s(\mu) = \frac{1}{b_0 \ln(\mu^2/\Lambda_n^2)} \left[1 - \frac{b_1 \ln \ln(\mu^2/\Lambda_n^2)}{b_0^2 \ln^2(\mu^2/\Lambda_n^2)} \right] \quad (3.1)$$

where b_0 and b_1 are given in Eq. (2.7). The value of the strong coupling constant thus depends on the number of active flavours. The matching of the coupling constant for different numbers of active flavours is made at the values $\mu = m$ where m is the mass of the charm, bottom or top quark. Following ref. [21] I shall choose the value of Λ_5 to lie in the range 100 – 250 MeV. The corresponding values of Λ for other numbers of active flavours is given in Table 1.

With this range of Λ_5 the spread in the value of the coupling constant at $\mu = 60$ GeV is determined to be $0.111 \leq \alpha_s(\mu = 60\text{GeV}) \leq 0.128$. This lack of determination of α_s gives an idea of the uncertainty to be expected in the prediction of top quark cross sections.

We now turn to the question of the choice of scale μ . Let us first consider the case of top quark production at the energy of the two presently operating $p\bar{p}$ colliders.

Λ_3 MeV	Λ_4 MeV	Λ_5 MeV
203	160	101
312	260	173
414	360	250

Table 1: Corresponding values of Λ_n with n active flavours.

The sensitivity to the choice of the scale μ is considerably reduced after inclusion of higher order terms. In Fig. 6 the cross section for the production of a putative top quark of mass 60 GeV is shown at CERN collider energies. The corresponding result at Fermilab energies is shown in Fig. 7. The inclusion of the $O(\alpha_s^3)$ corrections increases the reliability of the theoretical prediction since the sensitivity to the scale choice μ is reduced.

The overall conclusion for the case of the top quark is shown in Fig. 8, which shows the inclusive cross-section for the production of a t or a \bar{t} . The contributions coming from the decay $W^+ \rightarrow t\bar{b}$ and $W^- \rightarrow \bar{t}b$ have been included using the measured W cross-sections. The scale and parton distribution uncertainties are estimated using the extreme values of the DFLM distributions as shown in Fig. 8. As a result of the α_s^3 calculations the UA1 limits[2] on the masses of new heavy quarks have been revised[21]. They are now given by $m_t > 41$ GeV and $m_b > 34$ GeV. From this limit and Fig. 8 one can estimate that about 1000 t or \bar{t} events need to be produced in order to set a limit. Based on this number one can extrapolate to the likely discovery limit on the top quark in the upcoming runs at CERN and FNAL. With 1 pb^{-1} at $\sqrt{S} = 1.8$ TeV or 10 pb^{-1} at $\sqrt{S} = 0.63$ TeV one should be able to discover a top quark with a mass less than 80 GeV.

In contrast to the case of the top quark, phenomenological analysis of bottom quark production at collider energies is troublesome. The scale dependence of the cross-sections is extremely severe. This is illustrated in Figs. 9 and 10 where the scale dependence of the bottom quark cross-sections is shown before and after the inclusion of the higher order terms. The inclusion of the higher order corrections substantially modifies the cross section and aggravates the dependence on the scale μ . These cross-sections are uncertain for two reasons. Firstly, because the mass of the bottom quark is much smaller than the mass of the top quark, the coupling constant is bigger and

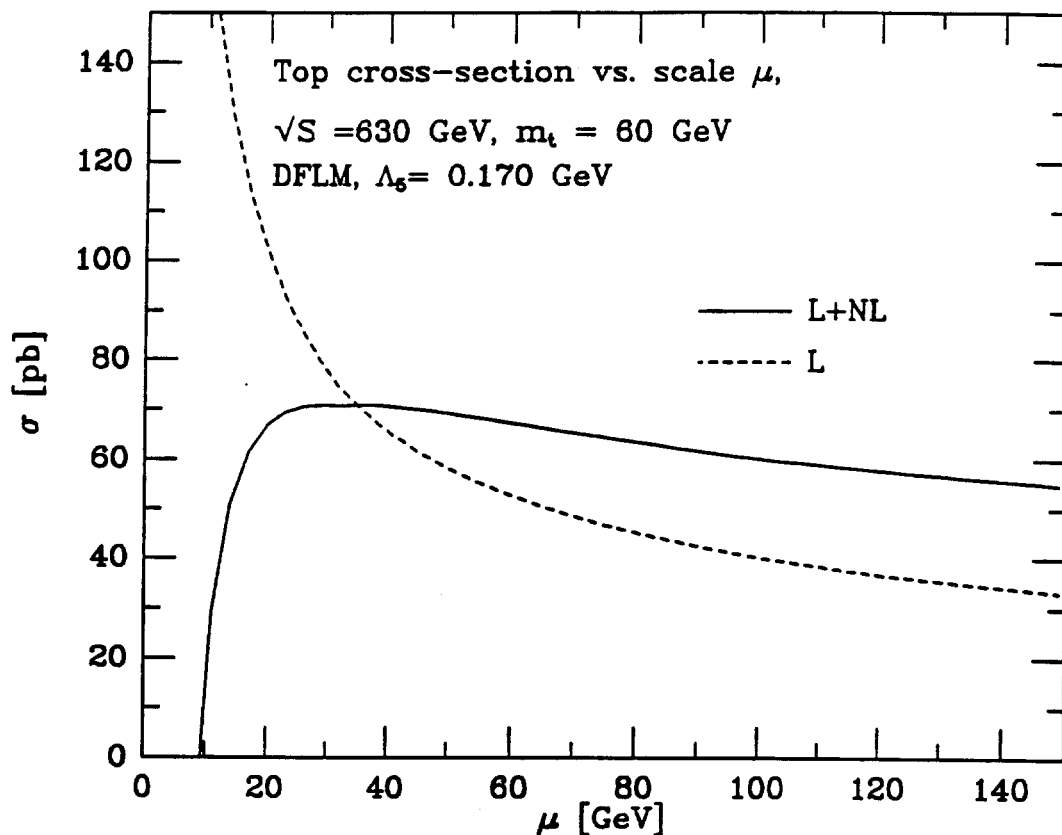


Figure 6: The total heavy quark cross section vs μ at $\sqrt{S} = 0.63$ TeV.

the significance of higher order terms (especially for the gluon-gluon subprocess) is greater. Secondly, in the limit of large S at fixed m , logarithmic effects of the form $\ln(S/m^2)$ become important and should be re-summed. These effects are due to the constant region in parton cross-sections discussed in section 2. It is therefore encouraging to note that despite these large theoretical uncertainties, the values measured by the UA1 collaboration[22] agree with the theoretical predictions[21].

$$\begin{aligned}
 \sigma(p\bar{p} \rightarrow b\bar{b} + X) &= 10.2^{+3.3}_{-3.3} \mu b && \text{UA1 data} \\
 \sigma(p\bar{p} \rightarrow b\bar{b} + X) &= 19^{+10}_{-8} \mu b && \text{Theory prediction, } m = 4.5 \text{ GeV} \\
 \sigma(p\bar{p} \rightarrow b\bar{b} + X) &= 12^{+7}_{-4} \mu b && \text{Theory prediction, } m = 5.0 \text{ GeV}
 \end{aligned}
 \tag{3.2}$$

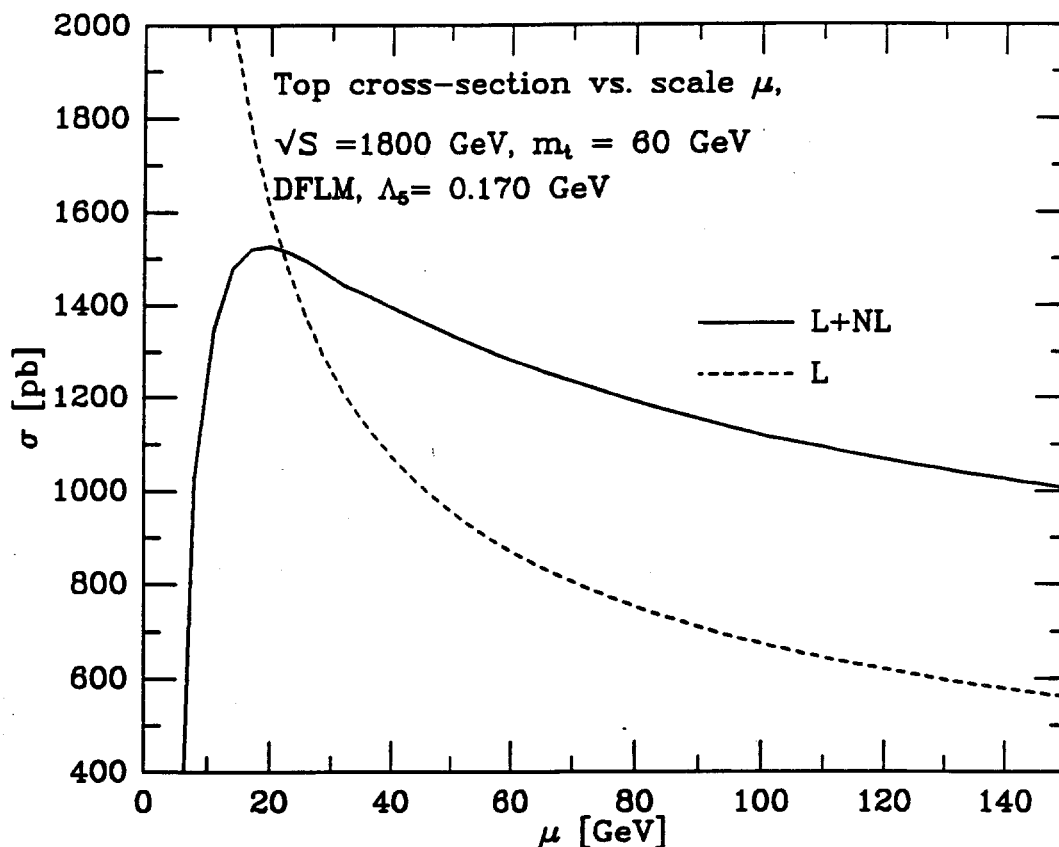


Figure 7: The total heavy quark cross section vs. μ at $\sqrt{S} = 1.8$ TeV.

4. The differential cross-section

In this section I present phenomenological results on the differential cross-section. The theoretical results on the one particle inclusive cross-section allow us to investigate the p_T and rapidity distributions of the produced heavy quarks. As an example in Fig. 11 I show the p_T distribution at the energy of the Tevatron. The shape of the differential cross section is significantly altered by the inclusion of higher order corrections. This qualitative feature remains true at all energies, both for bottom and top quarks.

The second, and as yet not yet completely resolved question, is the form of the p_T distribution when the p_T is very much larger than the mass m . This is obviously important since bottom quarks produced in this region provide a background for the top

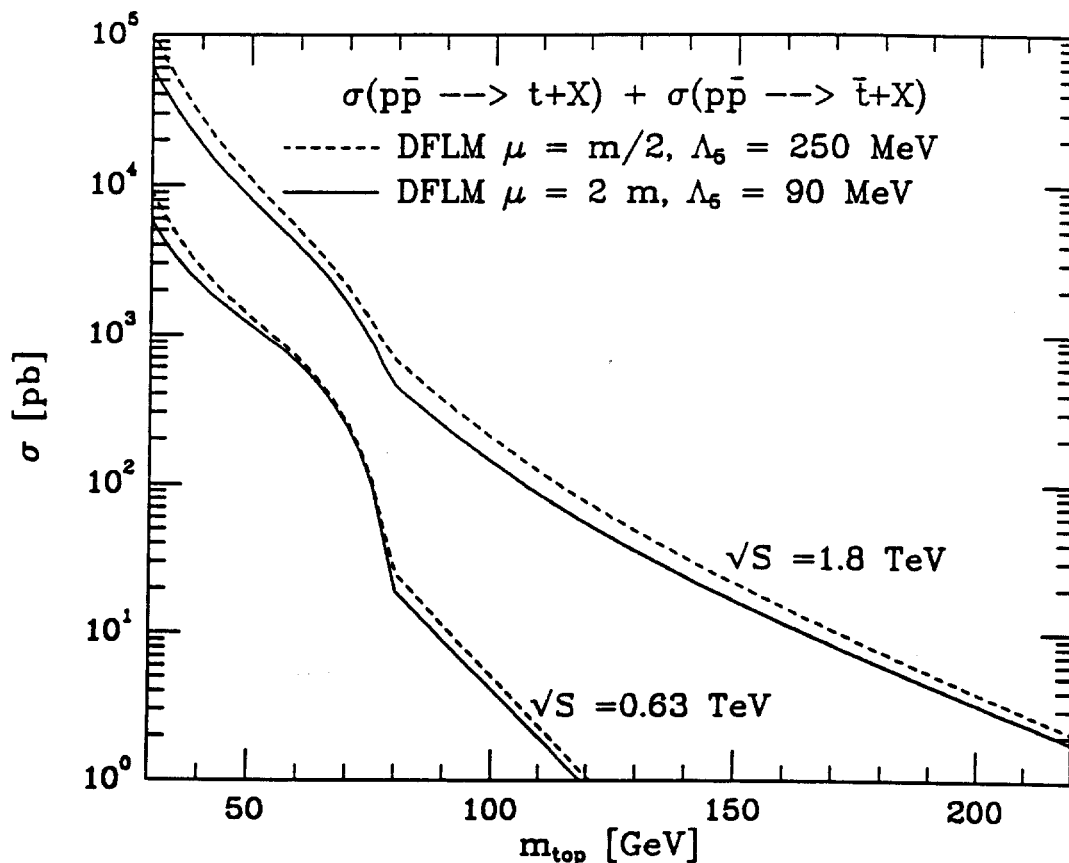


Figure 8: The inclusive cross section for the production of a top quark as a function of the mass m .

quark. In this kinematic region we encounter terms of the form $\alpha_s^{n+2} \ln^n(p_T^2/m^2)$ which should be summed before a reliable prediction can be obtained. The origin of these logarithms is well understood. They are the well known mass singularities arising from collinear divergences. The diagrams responsible for these mass singularities in order α_s^3 are shown in Fig. 12. Higher order logarithmic terms arise from the emission of additional collinear partons. Techniques exist to resum these logarithms, although this has not yet been performed. In order to make a prediction I will take the full result including $O(\alpha_s^3)$ terms evaluated at a scale $\mu = \sqrt{(p_T^2 + m^2)}$ with $m = 4.75 \text{ GeV}$ and $\Lambda_s = 160 \text{ MeV}$ with the structure functions of ref. [20] as a central value prediction. The error on this central value was estimated by adding in quadrature the modifications associated with the changes $\mu \rightarrow 2\mu \div \mu/2$, $\Lambda_s \rightarrow 90 \div 250 \text{ MeV}$ and

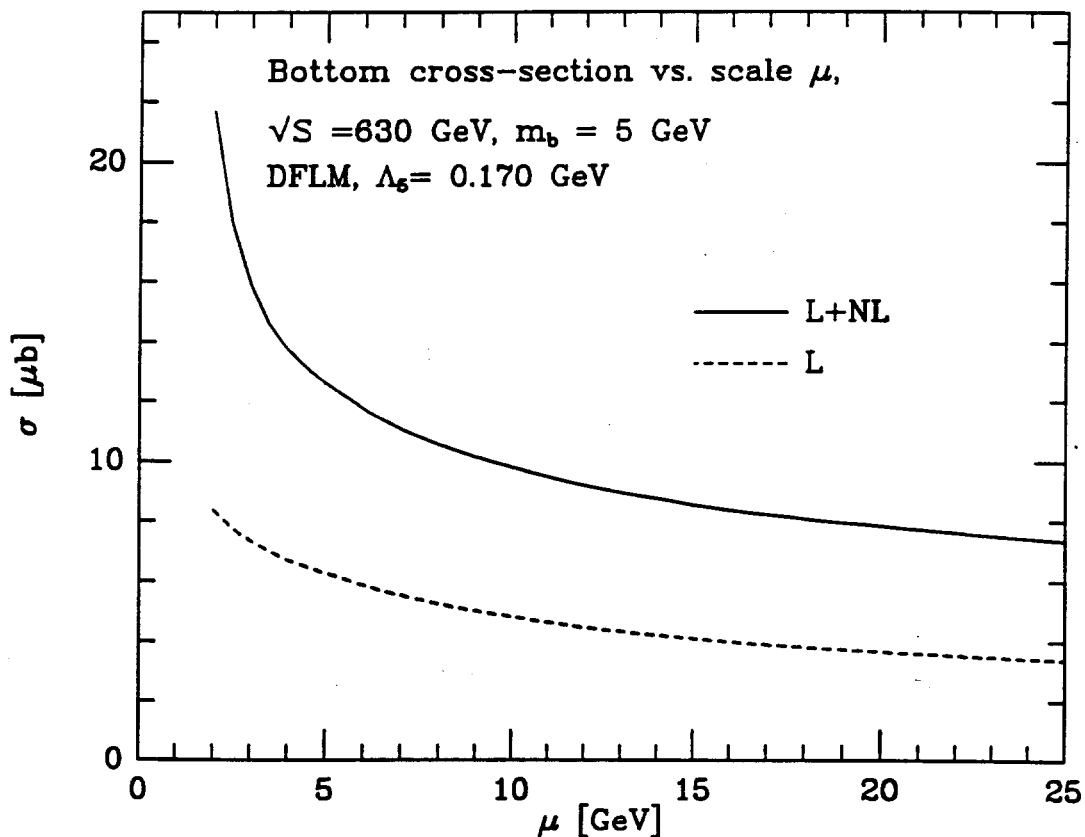


Figure 9: The total bottom quark cross section vs. μ at $\sqrt{S} = 0.63 \text{ TeV}$.

$m \rightarrow 4.5 \div 5.0 \text{ GeV}$. The contribution obtained by the addition of one more collinear parton is also estimated using the leading logarithmic approximation. It was used as an estimate of the error associated with logarithmic effects and added in quadrature to the errors already mentioned.

The UA1 experiment measures the cross-section for the inclusive production of bottom with a rapidity and p_T cut. Fig. 13 shows the theoretical prediction with the same rapidity and p_T cuts compared with the data. The dashed curve shows the theoretical error estimate calculated as indicated above. The agreement between theory and experiment is reasonably good, although the the data at high p_T lies above the theoretical prediction.

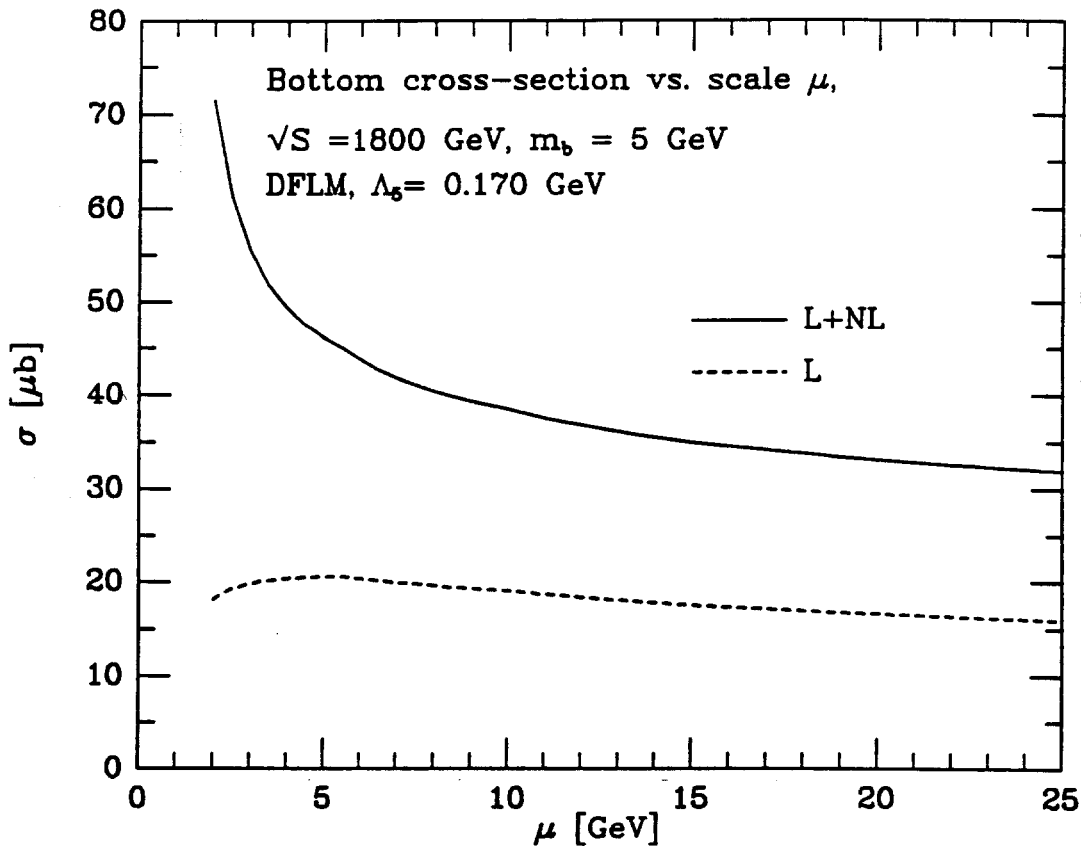


Figure 10: The total bottom quark cross section vs. μ at $\sqrt{S} = 1.8$ TeV.

5. Conclusion

There has been considerable progress in the theory of heavy quark production. The calculation of the strong radiative corrections has sharpened the theoretical estimates for the rate of top quark production at collider energies. For bottom quark production, the radiative corrections are very large and there is consequently a large uncertainty on the magnitude of the predicted cross section.

The shape of the one heavy quark differential distributions are not substantially modified by the inclusion of radiative corrections. The predicted differential distribution for bottom production at the $S\bar{p}\bar{p}S$ collider is in fair agreement with the UA1 results. It will be interesting to see how the p_T and rapidity distributions of the top quark compare with theory.

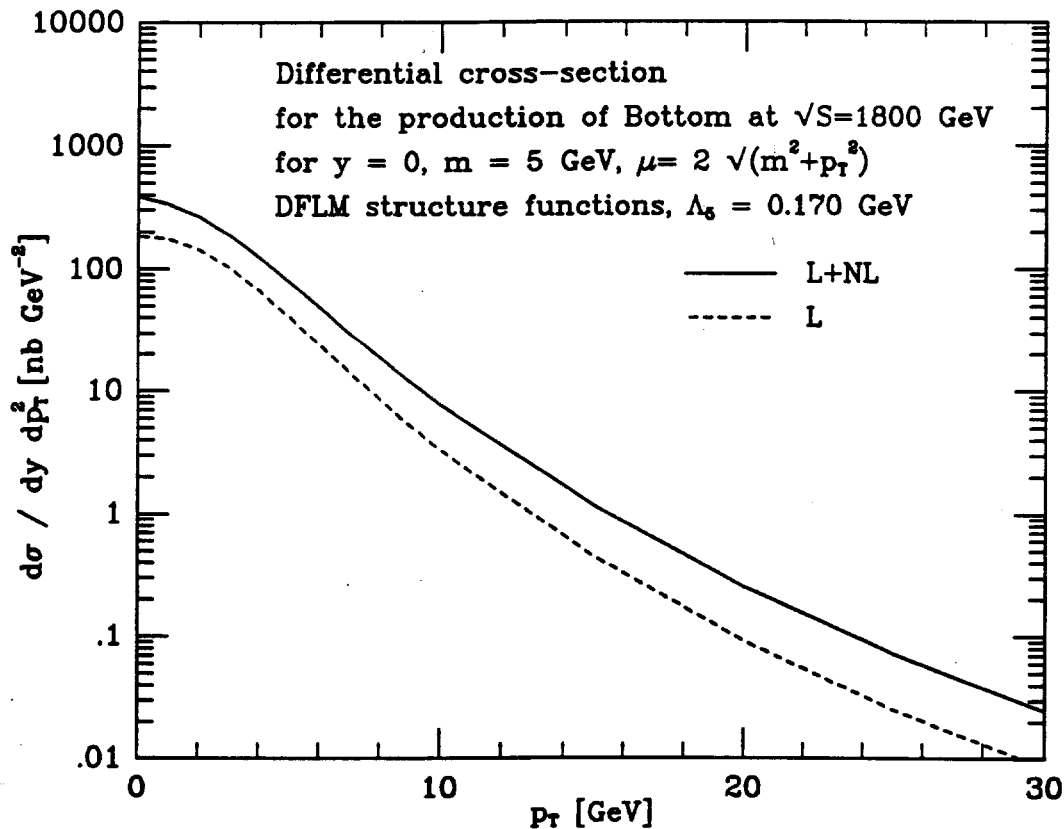


Figure 11: Leading and non-leading contributions to bottom quark production.

Acknowledgement.

The work described in this report was performed in collaboration with S. Dawson and P. Nason. I am indebted to them for many informative discussions of the material in this article.

References

- [1] S. P. K. Tavernier, *Rep. Prog. Phys.* **50** (1987) 1439 .
- [2] C. Albajar, *et al.*, *Zeit. Phys.* **C37** (1988) 505 .
- [3] J. C. Collins, D. E. Soper and G. Sterman, *Nucl. Phys.* **B263** (1986) 37 .

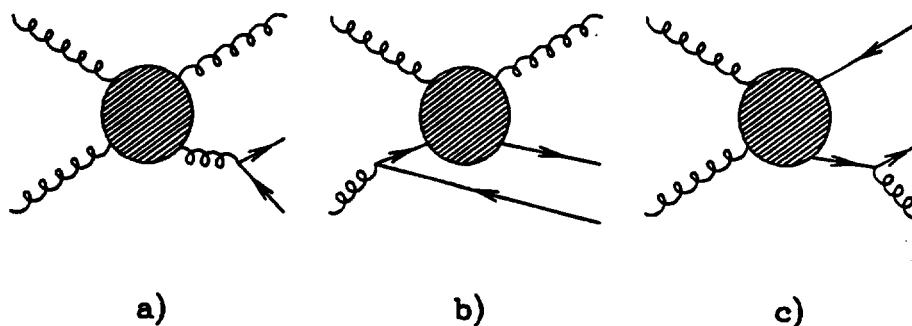


Figure 12: Diagrams giving logarithmic terms in third order.

- [4] S. J. Brodsky, J. C. Collins, S.D. Ellis, J. F. Gunion and A. H. Mueller, in *Proc. 1984 Summer Study on the Design and Utilization of the Superconducting Super Collider*, R. Donaldson and J. Morfin, (eds.), Fermilab, Batavia, Illinois, 1984, p. 227.
- [5] S. J. Brodsky, J. F. Gunion and D. E. Soper, *Phys. Rev.* **36** (1987) 2710 .
- [6] M. Gluck, J. F. Owens and E. Reya, *Phys. Rev.* **17** (1978) 2324 .
- [7] B. L. Combridge, *Nucl. Phys.* **B151** (1979) 429 .
- [8] R. K. Ellis, in *Strong Interactions and Gauge Theories*, edited by J. Tran Thanh Van, Editions Frontières, Gif-sur-Yvette, 1986, p. 339.
- [9] R. K. Ellis and C. Quigg, Fermilab preprint FN-445 (1987).

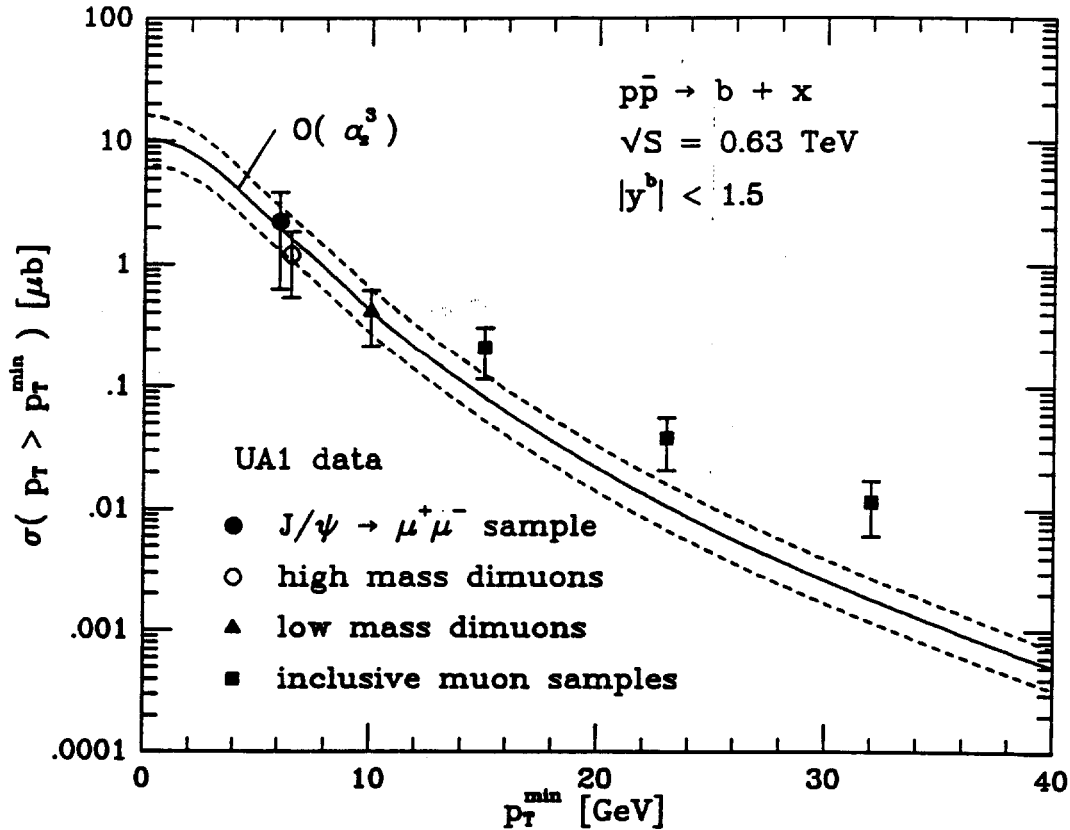


Figure 13: The theoretical prediction for bottom cross-section compared with UA1 data.

[10] Z. Kunszt and E. Pietarinen, *Nucl. Phys.* **B164** (1980) 45 .

[11] A. H. Mueller and P. Nason, *Phys. Lett.* **156B** (1985) 226 ;
Nucl. Phys. **B266** (1986) 265 .

[12] R. K. Ellis and J. C. Sexton, *Nucl. Phys.* **B282** (1987) 642 .

[13] J. F. Gunion and Z. Kunszt, *Phys. Lett.* **178B** (1986) 296 .

[14] R. K. Ellis and Z. Kunszt, *Nucl. Phys.* **B303** (1988) 653 .

[15] P. Nason, S. Dawson and R. K. Ellis, *Nucl. Phys.* **B303** (1988) 607 .

[16] W. Beenakker *et al.*, Leiden preprint (1988).

- [17] R. K. Ellis and P. Nason, Fermilab-Pub-88/54-T, (1988).
- [18] R. K. Ellis, Fermilab-Conf-88/73-T, (June 1988), *Proceedings of the Advanced Research Workshop on QCD Hard Hadronic Processes*, St. Croix, Virgin Islands, (October 1987).
- [19] D. Appel, G. Sterman and P. Mackenzie, Stonybrook preprint-ITP-SB-88-6 (1988).
- [20] M. Diemoz *et al.*, *Zeit. Phys.* **C39** (1988) 21 .
- [21] G. Altarelli *et al.*, *Nucl. Phys.* **B308** (1988) 724 .
- [22] C. Albajar *et al.*, CERN preprint, CERN-EP/88-100 (1988).

